# Lone-Pair Interfaces That Divide Inorganic Materials into Ionic and Covalent Parts**
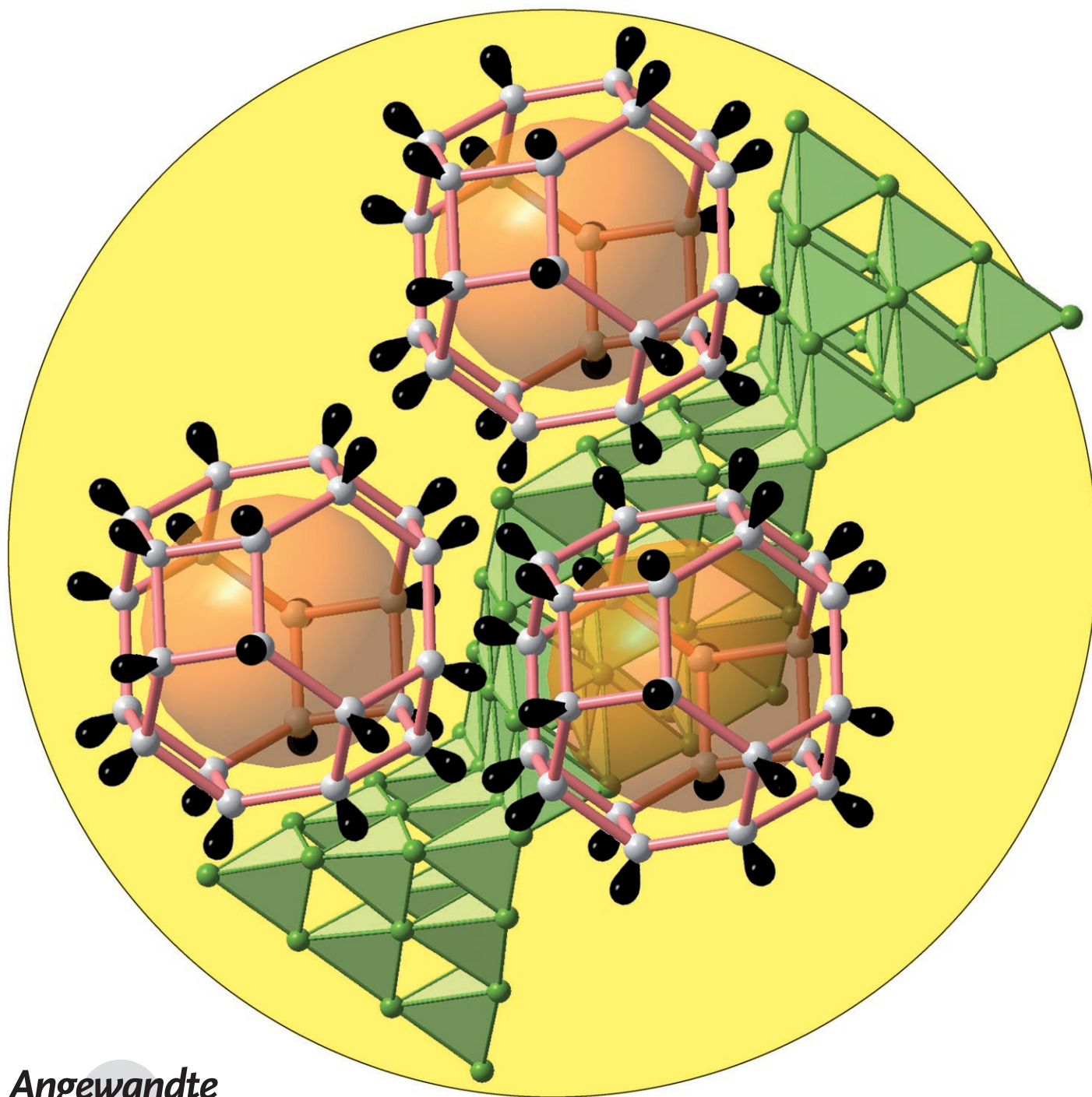
*Zuzana Mayerová, Mats Johnsson,\* and Sven Lidin*



*Angewandte*
*Chemie*

Compounds containing main-group metals in low oxidation states frequently exhibit stereochemically active lone pairs. In particular, this is observed for compounds of $Sn^{II}$, $Pb^{II}$, $As^{III}$, $Sb^{III}$, $Bi^{III}$, and $Te^{IV}$. An intriguing phenomenon is the localization of such lone pairs to well-defined regions of the solid-state structures of these compounds, wherein the volumes of lone pairs form surfaces that separate regions of different kinds of chemical interaction.[1–5] Interestingly, lone pairs tend to aggregate and even more so they tend to aggregate together with negatively charged ions. Here we show a striking example of how this segregation effect can be used to template solid-state compounds with reduced dimensionality.

The new compound $Cu_{20}Sb_{35}O_{44}Cl_{37}$ (**1**) crystallizes in the tetragonal space group *I4/mmm*, with unit-cell parameters $a = 18.144(2)$ Å and $c = 15.795(2)$ Å. It features extensive disorder, indicative of a lowering of local symmetry. Alternative descriptions were also extensively checked. Reciprocal space was explored to detect any additional scattering features, but neither classical superstructure reflections, incommensurate satellites, nor diffuse scattering was observed. We therefore conclude that the translational cell is correct. The disorder features may be taken as an indication of twinning or local disorder; to distinguish between the two, several low-symmetry models were evaluated and discarded in favor of our final high-symmetry choice. In that case, disorder appears to be strictly local in nature and is best modeled by using a split model and/or large displacement parameters for the disordered part.

The crystal structure of **1** consists of two distinct parts: edge-sharing $[Cu_{10}Cl_{16}]^{6-}$ T3 supertetrahedra (the edge of the supertetrahedron consists of the edges of three $CuCl_4$ tetrahedra) that form infinite chains, and isolated, octahedral $[Sb_{35}Cl_5O_{44}]^{12+}$ clusters with pseudo-cubic symmetry. A schematic overview of the structure is displayed in Figure 1. The two parts of the structure, namely an anionic part and a cationic part, are separated by an interface made up from the lone pairs associated with $Sb^{III}$. The lone pairs act as terminators for the Sb–O network, essentially by generating a nonbonding shell surrounding the large $(Sb_{35}Cl_5O_{44})^{12+}$ cluster. This illustrates a general feature of lone-pair oxohalide systems. A chalcophile partial structure terminates by a nonbonding lone-pair skin that faces a halide layer forming the surface of a halophile substructure. This phenomenon is also seen in, for example, $CuSb_2O_3Br$ and $CuSbTeO_3Cl_2$.[6–7] In the present case, the relatively halophilic Cu associates

[*] Z. Mayerová, Dr. M. Johnsson, Prof. Dr. S. Lidin
Department of Inorganic Chemistry
Stockholm University
106 91 Stockholm (Sweden)
Fax: (+46) 8152-187
E-mail: matsj@inorg.su.se

Supporting information for this article is available on the WWW under http://www.angewandte.org or from the author.



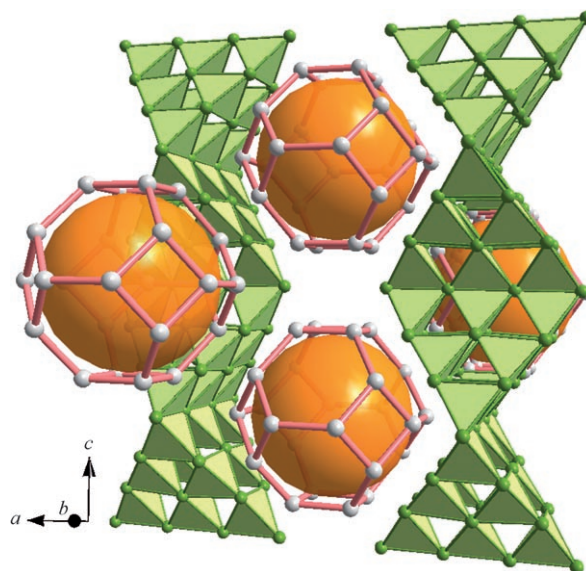**Figure 1.** Simplified view of the crystal structure for $Cu_{20}Sb_{35}O_{44}Cl_{37}$ (**1**) seen along the [010] axis. The covalently bonded clusters resembling zeolite β cages are placed in between sheets of ionically bonded supertetrahedra. Only Sb atoms (gray) and Cl atoms (green) are displayed. The orange spheres represent the void space within the clusters.

exclusively with Cl, while the chalcophile Sb associates with O atoms. The association of terminal Cl ions and lone pairs to an interface region in the structure is hardly the sign of any mutual attraction, but this cohabitation is rather the effect of the expulsion of nonbonding parts to the surface of a structural entity.

The Cu–Cl arrangement is simple but remarkable: $CuCl_4$ tetrahedra share Cl vertices to form T3 supertetrahedral $[Cu_{10}Cl_{20}]^{10-}$ units, much akin to the borosulfate and boroselenate T3 supertetrahedra reported by Krebs et al.[8–10] Recent research has focused on nanoclusters with large T$n$ supertetrahedral units, as they have a potential to create novel low-density nanoporous crystalline solids with many interesting properties. Those studies concern chalcogenide clusters built of supertetrahedra of type T4 and T5.[11–13] The largest T5 units are represented by pseudo-T5 clusters in $(Cu_5In_{30}S_{54})^{13-}$ or T5 tetrahedra found in $Na_{26}Mn_{39}O_{55}$.[12–13] Larger supertetrahedral units may be obtained by combining different T$n$ supertetrahedra and are known as supertetrahedra of supertetrahedra.[14] In all previously described compounds, the supertetrahedra are corner-sharing. The unique feature of the **1** is that the $[Cu_{10}Cl_{20}]^{10-}$ supertetrahedra share edges to form linear chains of the overall formulation $[(Cu_{10}Cl_{16})^{6-}]_\infty$. While edge-sharing is rather rare in tetrahedra, there is a facile local deformation mechanism for the accommodation of the accompanying strain in the T3 supertetrahedra that can clearly be seen in Figure 2. The Cu atoms that are located at the center of the three tetrahedra that form the edge of the supertetrahedron are displaced away from that edge towards the centre of the ensemble. The chains of supertetrahedra lie at the center of the isometric edges of the unit cell. Large cavities in the Cu–Cl packing are thus formed, which host the $[Sb_{35}Cl_5O_{44}]^{12+}$ clusters, centered at $\frac{1}{2}\frac{1}{2}0$ and at $00\frac{1}{2}$.
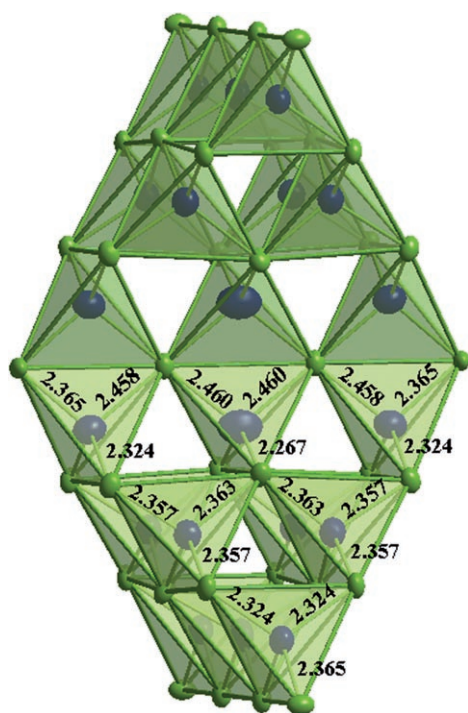
**Figure 2.** Each supertetrahedron consists of 10 CuCl$_4$ distorted tetrahedra (Cu blue, Cl green). The distortion of the Cu–Cl bond lengths at the common edge of two supertetrahedra is shown. The Cu atoms are displaced away from that edge.



**Figure 3.** Detailed view of the pseudo-cubic antimony oxochloride cluster outer shell (Sb gray, Cl green, O red). The shell forms a truncated octahedron with Sb at all vertices and at the centers of all hexagonal faces. Together with the oxygen atoms at all mid-edge positions, this forms an Sb$_{32}$O$_{36}$ cage equivalent to a β cage. Owing to the rather restrictive geometry of Sb–O distances and O-Sb-O angles, the Sb positions on the hexagonal faces are all split into six positions. All square faces are capped by Cl ions, which together form a large octahedron. The orange sphere represents the void space within the cluster.

The pseudo-cubic antimony oxochloride cluster consists of two shells: an outer shell that forms a truncated octahedron with Sb atoms at all vertices, and at the centers of all hexagonal faces with oxygen at all mid-edge positions forming an Sb$_{32}$O$_{36}$ cage equivalent to the β cages usually found in zeolites such as sodalite and similar to that found in compounds with the idealized composition [(Te$_{32}$Ni$_{30}$X$_3$O$_{90}$)$^{5+}$(Ni$_4$X$_{13}$)$^{5-}$] (X = Cl, Br).[15–16] An idealized picture of this arrangement is shown in Figure 3. Owing to the rather restrictive geometry of Sb–O distances and O-Sb-O angles, the Sb positions on the hexagonal faces are all split into six positions. All square faces are capped by Cl ions, together forming a large octahedron. As a result of short distances along the *c* direction to neighboring clusters, the apical Cl positions are only half filled while the equatorial positions are all fully occupied. Within this large octahedral shell dwells the second entity, an O$_8$ cube capped on all faces by Sb with almost-half occupancies. In the center of this unit, there is another Sb position with a relatively low occupancy (ca. 1/6). This arrangement, formally Sb$_7$O$_8$, but rather closer to Sb$_3$O$_8$ by composition, is shown in Figure 4. This inner part of the cluster is bonded to the partially occupied Sb atoms of the outer shell, generating a large number of possible configurations related by minor rotational adjustments. We modeled this part of the structure with split positions to generate admissible Sb–O distances. The central Sb atom was assumed to be distributed over several positions as well in response to the presence or absence of the six apical Sb atoms, but given the rather low occupancy and the high symmetry of this position it was deemed prudent to model this atom by
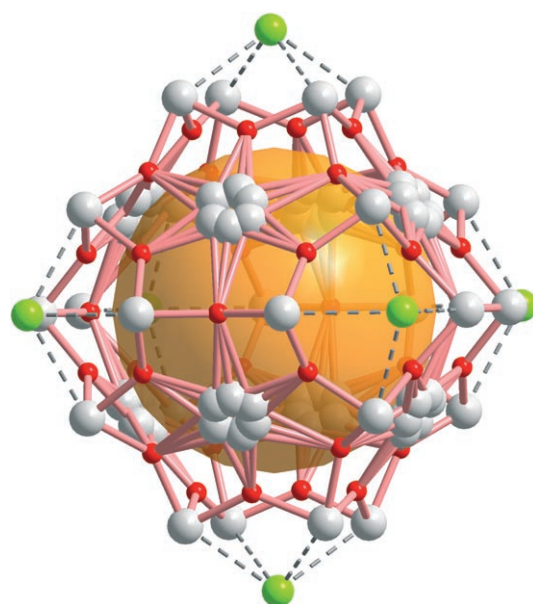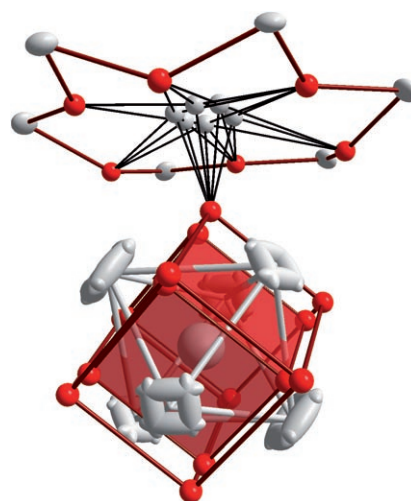


**Figure 4.** Relation between the outer and inner parts of the antimony oxochloride cluster. The two parts of the cluster are connected through the oxygen atoms of the inner shell and the six split Sb positions that lie at the center of the hexagonal planes of the outer shell. The oxygen positions are split to decrease the Sb–O strain in the outer layer. The inner part consists of a partly occupied central Sb atom surrounded by cubically arranged O atoms and an octahedron of partly occupied split Sb positions (Sb gray, O red).

using a single position. Because of the unconstrained partial occupancies, the total composition of the cluster was in fact Sb$_{34.67}$Cl$_5$O$_{44}$, while overall charge balance would dictate [Sb$_{35}$Cl$_5$O$_{44}$]$^{12+}$.

The Sb atoms that make up the β cages behave more or less as expected for $Sb^{III}$. The Sb atoms that occupy the vertices of the truncated octahedron form the apices of squat trigonal pyramids. Together with their stereochemically active lone pair (E), this makes up a set of $SbO_3E$ tetrahedra. If the Cl atoms that complete the octahedron are taken into account, the coordination is still an unsurprising $SbClO_3E$ trigonal bipyramid for these atoms. The Sb site at the center of the hexagonal window of the truncated octahedron is rather more troubled. This position is not ideally suited for an Sb atom, neither when considering distances nor when considering geometry. The result is a split of this position into six distinct locations, each with three suitable Sb–O distances within the hexagonal ring and one Sb–O distance to an oxygen atom that belongs to the entity in the center of the cluster. The general coordination is then, not unexpectedly, again a trigonal-bipyramidal $SbO_4E$, but this is rather strained having three oxygen atoms coplanar with the central Sb atom (such a coordination is also observed in $Sb_8O_{11}Cl_2$).[17] The coordination of the Sb atoms in the inner cluster is a $SbO_4E$ square pyramid (this type of coordination was previously observed for $Sb^{III}$ in, for example, the compound Ba-$SbO_2Cl$).[18]

It is still unclear if there is a positive interaction between lone-pair aggregates and negatively charged ions or if the agglomeration is simply an effect of mutual expulsion from the bonded regions of the structure. A simple but typical example is tetragonal BiOCl in which Bi and O form a covalently bonded oxidic sheet that terminates on both sides by layers of $Bi^{III}$ lone pairs. The Cl ions are found in the regions outside these sheets.[19] The Cl region of the structure may actually be intercalated by alkali metals as in $Cs_xBi_{2-x}Pb_xO_2Cl_2$ to form a second, ionically bonded sub-structure.[20] Lone pairs define the boundary between the two regions of different interactions.

In summary, lone pairs separate two structurally very different regions in the compound $Cu_{20}Sb_{35}O_{44}Cl_{37}$ (**1**) described. The halophile copper forms a relatively simple structure of edge-sharing T3 supertetrahedra that form infinite chains along the tetragonal *c* direction. Interspersed between these $[Cu_{10}Cl_{16}^{6-}]_\infty$ columns are covalent entities, namely $[Sb_{35}Cl_5O_{44}]^{12+}$ clusters. If the interconnectivity of the $[Cu_{10}Cl_{16}^{6-}]_\infty$ columns is ignored and the center of the supertetrahedra are considered as the loci of negatively charged clusters, the whole ensemble may be regarded as a fluorite-type packing of clusters. While the $[Cu_{10}Cl_{16}^{6-}]_\infty$ columns terminate by an outer layer of Cl ions, the $[Sb_{35}Cl_5O_{44}]^{12+}$ clusters present a surface covered by $Sb^{III}$ lone pairs, and in the typical fashion of lone-pair oxohalides, we find a dividing region; in this case, in the shape of undulating tubes built from lone pairs and halide ions.

### Experimental Section

$Sb_2O_3$ (Aldrich), CuCl (ABCR), $SbCl_3$ (ACROS organics), and amorphous $SiO_2$ (prepared by hydrolysis of TEOS (ACROS organics) and subsequent calcinations) were used as starting materials for the synthesis of $Cu_{20}Sb_{35}O_{44}Cl_{37}$ (**1**). A mixture of $SiO_2$, $Sb_2O_3$, and CuCl in 1:1:1 molar ratio was placed in a sealed evacuated silica tube and subsequently heat-treated in a muffle furnace at 500°C for 93 h. The product was a mixture of a yellow powder, transparent yellow crystals, and yellow-green single crystals of $Cu_{20}Sb_{35}O_{44}Cl_{37}$. As single crystals of **1** were found only in one end of the silica tubes, chemical transport appears to be involved in the growth mechanism. The crystals used for analyses were selected manually on the basis of color and morphology. The compound was also synthesized as a powder from a stoichiometric mixture of $Sb_2O_3/SbCl_3/CuCl$ (44:17:60).

Single-crystal X-ray diffraction data on **1** were collected at 290 K on an STOE IPDS diffractometer equipped with an image plate and graphite-monochromatized $Mo_{K\alpha}$ radiation ($\lambda = 0.71073$ Å) from a rotating anode. The intensities of the reflections were integrated by using the software provided by the manufacturer, and absorption correction was carried out numerically, after crystal shape optimization.[21–22] The structures were solved by direct methods (SHELXS97) and refined by full-matrix least squares on $|F|$ using the program Jana2000.[23–24] All illustrations were made with the program Diamond.[25] 24807 reflections, of which 1783 were unique, were collected in the region $2.24 < \theta < 27.98°$; space group $I4/mmm$; unit cell dimensions $a = 18.144(2)$ Å, $c = 15.795(2)$ Å, $Z = 2$, $V = 5199.37(99)$ Å$^3$. All fully occupied atomic positions except oxygen were refined using anisotropic displacement parameters. $R = 0.0639$ for 1.556 reflections with $I > 3\sigma(I)$ and 0.0714 for 1.783 reflections; $wR = 0.0997$ and $S = 1.83$ (the goodness of fit on $|F|$). Crystal data, details of structure determination, atomic coordinates, equivalent isotropic displacement parameters, and bond lengths are given in the Supporting Information. Further details on the crystal structural investigations may be obtained from the Fachinformationszentrum Karlsruhe, 76344 Eggenstein-Leopoldshafen, Germany (fax: (+ 49)7247-808-666; e-mail: crysdata@fiz-karlsruhe.de), on quoting the depository number CSD-416247.

The chemical composition of the products were confirmed by using energy-dispersive spectrometry (EDS, LINK AN10000) in a scanning electron microscope (SEM, JEOL 820). See Supporting Information for the measured chemical composition.

[1] H. Katzke, Y. Oka, Y. Kanke, K. Kato, T. Yao, *Z. Kristallogr.* **1999**, *214*, 284–289.

[2] C. Särnstrand, *Acta Crystallogr. Sect. B* **1978**, *34*, 2402–2407.

[3] W. Altenburger, W. Hiller, I. R. Jahn, *Z. Kristallogr.* **1987**, *181*, 227–234.

[4] J. A. Alonso, *J. Chem. Soc. Dalton Trans.* **1998**, *12*, 1947–1950.

[5] J. A. Alonso, E. Gutérrez-Puebla, A. Jerez, A. Monge, C. Ruiz-Valero, *J. Chem. Soc. Dalton Trans.* **1985**, 1633–1635.

[6] Z. Mayerová, M. Johnsson, S. Lidin, *J. Solid State Chem.* **2005**, *178*, 3487–3491.

[7] R. Becker, M. Johnsson, R. Kremer, P. Lemmens, *Solid State Sci.* **2003**, *5*, 1411–1416.

[8] A. Hammerschmidt, P. zum Hebel, F. Hiltmann, B. Krebs, *Z. Anorg. Allg. Chem.* **1996**, *622*, 76–84.

[9] B. Krebs, H. Diercks, *Z. Anorg. Allg. Chem.* **1984**, *518*, 101–114.

[10] P. zum Hebel, B. Krebs, M. Gruene, W. Mueller-Warmuth, *Solid State Ionics* **1990**, *43*, 133–142.

[11] C. Wang, Y. Li, X. Bu, N. Zheng, O. Zivkovic, C.-S. Yang, P. Feng, *J. Am. Chem. Soc.* **2001**, *123*, 11506–11507.

[12] X. Bu, N. Zheng, Y. Li, P. Feng, *J. Am. Chem. Soc.* **2002**, *124*, 12646–12647.

[13] A. Möller, P. Amann, V. Kataev, N. Schitter, *Z. Anorg. Allg. Chem.* **2004**, *630*, 890–894.

[14] H. Li, J. Kim, M. O'Keeffe, O. M. Yaghi, *Angew. Chem.* **2003**, *115*, 1863–1865; *Angew. Chem. Int. Ed.* **2003**, *42*, 1819–1821.

[15] L. Pauling, *Z. Kristallogr. Kristallgeom. Kristallphys. Krista* **1930**, *74*, 213–225.

[16] M. Johnsson, S. Lidin, K. W. Törnroos, H.-B. Bürgi, P. Millet, *Angew. Chem.* **2004**, *116*, 4292–4295; *Angew. Chem. Int. Ed.* **2004**, *43*, 4292–4295.

[17] S. Menchetti, C. Sabelli, R. Trosti-Ferroni, *Acta Crystallogr. Sect. C* **1984**, *40*, 1506–1510.

[18] F. Thuillier-Chevin, P. Maraine, G. Perez, *Rev. Chim. Miner.* **1980**, *17*, 102–109.

[19] F. A. Bannister, *Mineral. Mag. J. Mineral. Soc.* **1935**, *149*, 49–58.

[20] D. O. Charkin, P. S. Berdonosov, A. M. Moisejev, R. R. Shagiakhmetov, V. A. Dolgikh, P. Lightfoot, *J. Solid State Chem.* **1999**, *147*, 527–535.

[21] X-RED, Version 1.07, STOE & Cie GmbH, Darmstadt, Germany, **1996**.

[22] X-SHAPE revision 1.09, STOE & Cie GmbH, Darmstadt, Germany, **1997**.

[23] G.-M. Sheldrick, SHELXS-97—Program for the Solution of Crystal Structures, Göttingen, **1997**.

[24] V. Petříček, M. Dusek, Institute of Physics AVCR, Praha, Czech Republic, **2000**.

[25] K. Brandenburg, DIAMOND Release 2.1e, Crystal Impact GbR, Bonn, Germany, **2000**.